STEM CELLS TRANSLATIONAL MEDICINE®

ENABLING TECHNOLOGIES FOR CELL-BASED CLINICAL TRANSLATION

# Survival and Functionality of Human Induced Pluripotent Stem Cell-Derived Oligodendrocytes in a Nonhuman Primate Model for Multiple Sclerosis

ARUN THIRUVALLUVAN,[a] MARCIN CZEPIEL,[a] YOLANDA A. KAP,[c] IETJE MANTINGH-OTTER,[a] ILIA VAINCHTEIN,[a] JEROEN KUIPERS,[b] MARJOLEIN BIJLARD,[b] WIA BARON,[b] BEN GIEPMANS,[b] WOLFGANG BRÜCK,[d] BERT A. 'T HART,[a,c] ERIK BODDEKE,[a] SJEF COPRAY[a]

**Key Words.** Oligodendrocytes • Multiple sclerosis • Nonhuman primates • Myelination

Departments of [a]Neuroscience and [b]Cell Biology, University Medical Centre Groningen, University of Groningen, Groningen, The Netherlands; [c]Department of Immunobiology, Biomedical Primate Research Centre, Rijswijk, The Netherlands; and [d]Department of Neuropathology, University Medical Centre Göttingen, Göttingen, Germany

Correspondence: Sjef Copray, Ph.D., Department of Neuroscience, University Medical Center Groningen, A. Deusinglaan 1, 9713 AV, Groningen, The Netherlands. Telephone: 31-50-3632758; E-Mail: j.c.v.m.copray@umcg.nl

Received January 14, 2016; accepted for publication April 7, 2016; published Online First on July 11, 2016.


1066-5099/2016/$20.00/0

http://dx.doi.org/10.5966/sctm.2016-0024

## ABSTRACT

**Fast remyelination by endogenous oligodendrocyte precursor cells (OPCs) is essential to prevent axonal and subsequent retrograde neuronal degeneration in demyelinating lesions in multiple sclerosis (MS). In chronic lesions, however, the remyelination capacity of OPCs becomes insufficient. Cell therapy with exogenous remyelinating cells may be a strategy to replace the failing endogenous OPCs. Here, we differentiated human induced pluripotent stem cells (hiPSCs) into OPCs and validated their proper functionality in vitro as well as in vivo in mouse models for MS. Next, we intracerebrally injected hiPSC-derived OPCs in a nonhuman primate (marmoset) model for progressive MS; the grafted OPCs specifically migrated toward the MS-like lesions in the corpus callosum where they myelinated denuded axons. hiPSC-derived OPCs may become the first therapeutic tool to address demyelination and neurodegeneration in the progressive forms of MS.** STEM CELLS TRANSLATIONAL MEDICINE *2016;5:1550–1561*

## SIGNIFICANCE

This study demonstrates for the first time that human induced pluripotent stem cell (iPSC)-derived oligodendrocyte precursor cells (OPCs), after intracortical implantation in a nonhuman primate model for progressive multiple sclerosis (MS), migrate to the lesions and remyelinate denuded axons. These findings imply that human iPSC-OPCs can be a therapeutic tool for MS. The results of this feasibility study on the potential use of hiPSC-derived OPCs are of great importance for all MS researchers focusing on the stimulation of remyelination in MS patients. Further optimization and research on practical issues related to the safe production and administration of iPSC-derived cell grafts will likely lead to a first clinical trial in a small group of secondary progressive MS patients. This would be the first specific therapeutic approach aimed at restoring myelination and rescuing axons in MS patients, since there is no treatment available for this most debilitating aspect of MS.

## INTRODUCTION

Multiple sclerosis (MS) is a devastating disease of the central nervous system (CNS) characterized by inflammation, loss of myelin, axonal and neuronal degeneration, and progressive brain atrophy [1]. MS is generally considered an autoimmune disease, manifesting itself in most patients by a relapsing-remitting course (RRMS) [2]. During the relapse phase of RRMS, autoreactive T cells invade the CNS and trigger myelin degradation and oligodendrocyte death. During the remission phase, much of the myelin damage is restored by endogenous oligodendrocyte precursor cells (OPCs). New insights tend to consider MS as a continuously progressing, neurodegenerative disorder, over which a fluctuating aberrant autoimmune response is superimposed. The relapses do not affect the underlying continuation of neurodegeneration, which becomes overt again in the relapse-free secondary progressive state [3]. In line with this view is the observation that many novel potent anti-inflammatory drugs can delay or even eliminate relapses in RRMS but are still unable to stop the transition to the secondary progressive phase. In this novel perspective on MS, primary progressive MS, lacking inflammatory relapses, is the "purest" form of the disorder [3]. In the (secondary) progressive phase, which typically develops at an advanced age, endogenous OPCs are no longer able to restore myelin to prevent neurodegeneration and, with that, loss of neurological function. Novel therapies for chronic progressive types of MS should focus on arresting neurodegeneration and providing neuroprotection,

with the most effective protection offered by rapid axonal remyelination. Cell-based remyelination therapy has been considered a valid approach [4]. Several sources for exogenous, transplantable OPCs have been proposed; oligodendrocyte precursors have been generated from neural stem cells (NSCs) [5] and embryonic stem cells (ESCs). The potential clinical application of both cell types in MS, however, is problematic. Sources of NSCs are difficult to access, and NSCs appear to be restricted in their proliferation and differentiation potential, whereas the use of ESCs raises ethical concerns. Moreover, OPCs derived from both of these nonautologous cell sources would be attacked by the host immune system and inevitably rejected after implantation. A therapy using these cells would need to be accompanied by immunosuppressive treatment.

In 2006, the phenomenon of induced pluripotency was first described [6]. Lacking the disadvantages of NSCs and ESCs, induced pluripotent stem cells (iPSCs) have become intensively studied as a potential, novel source of patient-specific cell types for disease modeling and autologous cell-based therapies. A few studies have demonstrated that human iPSCs can be differentiated into OPCs and produce myelin basic protein (MBP) [7–11]. The functionality and clinical potential of these human iPSC-derived OPCs were proven after transplantation in a rat model for optic nerve demyelination [8] and in newborn shiverer mice [9, 10]. Moreover, human iPSC-derived OPCs grafted into irradiated rats appeared to be effective in restoring myelin damage caused by radiation [12]. None of the animal models above represents the autoimmune condition of the inflammatory-demyelinated lesion in MS [13].

In the present study, we examined for the first time the fate and functionality of human iPSC-derived OPCs after implantation in a nonhuman primate model of MS. After verifying the validity of our human iPSC-OPC differentiation protocol and the functionality of these OPCs in vitro and in vivo in two mouse models, we stereotactically injected suspensions of human iPSC (hiPSC)-derived OPCs into the cerebral cortex of marmosets with experimental autoimmune encephalomyelitis (EAE). We induced EAE in the marmoset monkeys by immunization with a synthetic peptide representing residues 34 to 56 of human myelin oligodendrocyte glycoprotein ($MOG_{34–56}$) [14]. This specific primate EAE model is considered the best animal model of MS, as it approximates progressive disease in clinical and pathological presentation. Important for the present study is the occurrence of typical demyelinated, inflammatory lesions resembling those found in the brains of MS patients. We demonstrate that implanted human iPSC-derived OPCs survive and migrate toward MS-like lesions in the corpus callosum, where they differentiate into myelin-forming mature oligodendrocytes.

## Materials and Methods

### Differentiation of hiPSCs Toward Oligodendrocytes

For the differentiation of hiPSCs into oligodendrocytes, a five-stage protocol was developed: (a) generation of primitive neuroepithelial cells, (b) specification of Olig2 progenitor cells, (c) generation of pre-OPCs, (d) maturation of pre-OPCs to OPCs, and (e) differentiation of OPCs on substrate. A detailed description of the various culture conditions for each stage may be found in the supplemental online data.

At defined time points (e.g., every 2 weeks) some of the floating hiPSC-derived spheres were seeded onto coverslips coated with polyornithine/laminin (20 $\mu$g/ml) to check for the identity of the cells migrating out of the cell clusters. At this stage, cells were cultured in the medium described for Stage 4. The number of OPCs migrating out typically increased over time; on average, it took around 140–150 days to complete the protocol, resulting in a cell population of OPCs with a purity of 75% as determined by immunohistochemistry (almost all other cells being NSCs). From each stage, cells were fixed with 4% PFA and immunocytochemically stained to verify cell identity and control the differentiation progress.

### Cocultures of hiPSC-Derived OPCs and Dorsal Root Ganglion Neurons

To examine the myelinating capacity of hiPSC-derived OPCs in vitro, they were cocultured with rat dorsal root ganglion (DRG) neurons. DRG neurons were dissected from 15-day-old Wistar rat embryos and digested in papain (1.2 U/ml; Sigma-Aldrich, St Louis, MO, http://www.sigmaaldrich.com), L-cysteine (0.24 mg/ml; Sigma-Aldrich), and DNase I (40 mg/ml; Roche, Basel, Switzerland, http://www.roche.com) for 1 hour at 37°C. The dissociated cells were plated at a density of 60,000 cells per 13-mm coverslip precoated with 5 $\mu$g/ml polylysine/laminin and Matrigel Growth Factor Reduced (1:40 dilution). DRG neurons were cultured for 21 days in Dulbecco's modified Eagle's medium (Thermo Fisher Scientific Life Sciences, Waltham, MA, http://www.thermofisher.com) supplemented with 10% fetal calf serum (FCS) (Bodinco, Alkmaar, The Netherlands, http://www.bodinco.nl; L-glutamine) and penicillin/streptomycin in the presence of nerve growth factor (100 ng/ml). Cells were pulsed four times for 2 days with fluorodeoxyuridine (10 $\mu$M) to remove contaminating proliferating cells, in particular fibroblasts and Schwann cells. The purity of the DRG culture was microscopically confirmed. Subsequently, approximately 25,000 hiPSC-derived OPCs were seeded onto coverslips containing the DRG neurons with extensive axonal outgrowth. The following day, the medium was changed to glia medium without platelet-derived growth factor AA (PDGF-AA). OPCs were cocultured with the DRG neurons for 28 days, with medium change every second day. After that period, cultures were fixed with 4% paraformaldehyde (PFA) and immunostained for MBP and neurofilament (NF).

### EAE Induction in the Common Marmoset

Four adult (female, age 2–5 years) common marmosets (*Callithrix jacchus*) were obtained from the purpose-bred colony at the Biomedical Primate Research Centre (Rijswijk, The Netherlands). Only marmosets that were declared healthy after the veterinarian's physical, hematologic, and biochemical check-up were included in the study. Monkeys were pair-housed in spacious cages and remained under intensive veterinary supervision throughout the study. The daily diet consisted of commercial food pellets for New World monkeys (Special Diet Services, Witham, Essex, UK, http://www.sdsdiets.com), supplemented with raisins, peanuts, marshmallows, biscuits, and fresh fruit. Drinking water was provided ad libitum.

All experimental procedures were reviewed and approved by the Institute's Animal Ethics Committee, and animals were housed and handled according to Dutch Law in animal experimentation. The animal facilities of the Biomedical Primate Research Centre have been inspected and accredited by Association for Assessment and Accreditation of Laboratory Animal Care International. EAE in marmosets was induced with a synthetic peptide representing amino acids 34–56 of human myelin oligodendrocyte glycoprotein

 

($MOG_{34–56}$; sequence = GMEVGWYRPPFSRVVHLYRNGKD; Cambridge Research Biochemicals Limited, Cleveland, UK, http://www.crbdiscovery.com) emulsified in incomplete Freund's adjuvant (IFA) (BD, Detroit, MI, http://www.bd.com). The inoculum contained 100 $\mu$g $MOG_{34–56}$ in 200 $\mu$l phosphate-buffered saline (PBS) and was emulsified in 200 $\mu$l IFA by gentle stirring for at least 1 hour at 4°C. The emulsion was injected as 4 spots of 100 $\mu$l into the dorsal skin, 2 in the axillary and 2 in inguinal region under sedation by alfaxalone (10 mg/kg alfaxan; Vetoquinol, Den Bosch, The Netherlands, http://www.vetoquinol.nl), with booster immunizations occurring every 28 days until development of overt neurological disease (EAE score $\geq$2) was observed. Clinical signs were scored daily by two independent observers using a previously described semiquantitative scale [15]. Briefly, 0 = no clinical signs; 0.5 = apathy, altered walking pattern without ataxia; 1 = lethargy, tail paralysis, tremor; 2 = ataxia, optic disease; 2.25 = monoparesis; 2.5 = paraparesis, sensory loss; 3 = para- or hemiplegia. Overt neurological deficit starts at score 2. For ethical reasons, monkeys were sacrificed once paresis of one or more limbs (score $\geq$2.5) was observed. Body weight measurements of conscious monkeys, which is used a surrogate disease marker, were performed twice per week).

### Stereotactic Procedure in the Common Marmoset

hiPSC-derived OPCs were injected above the corpus callosum of marmosets via a stereotactic procedure 79 days after immunization. Animals were sedated by alfaxan and received buprenorphine (Buprecare, 0.3 mg/ml buprenorphine base, 20–100 $\mu$g/kg; Schering-Plough, Maarssen, The Netherlands, http://www.schering-plough.com) as analgesic. Differentiated hiPSC-derived OPCs were transfected with episomal green fluorescent protein (GFP) (pCXLE-EGFP) for 4–6 hours with FuGENE HD and refreshed with OPC medium. Episomal GFP-labeled hiPSC-derived-OPCs were gently detached from the substrate using Accutase, spun down, and resuspended in PBS at a concentration of 12,500 cells per microliter, and 4 $\mu$l of cell suspension was stereotactically injected using the following coordinates in relation to the bregma: anterior-posterior, 3.8; lateral, 2.5; vertical, 8; 20-degree angle, 16. Injection speed was kept at 2 $\mu$l of cell suspension per minute followed by 5 minutes of deposition time before needle retraction. To prevent immune rejection of the xenografts, the marmosets received cyclosporine A (Sandimmune, Novartis, Basel, Switzerland, http://www.novartis.com) once daily by intramuscular injection of 10 mg/kg, starting 1 day before the stereotactic procedure.

To follow the fate (survival, migration, and differentiation) of the grafted OPCs, we planned to perfuse and fixate the marmosets with 4% PFA under alfaxan and ketamine anesthesia at four time points after implantation: 10, 20, 30, or 40 days. Ethical restrictions did not allow us to follow EAE-affected marmosets for more than 40 days. Brain and spinal cord were stored in formalin for 2 weeks and then transferred into PBS, further sectioned (16-$\mu$m cryosections), and prepared for immunohistochemical and histological analysis.

### Immunochemistry

PFA-fixed cells or tissue slices were washed two times with PBS. Nonspecific antibody binding sites were blocked with PBS+ (PBS containing 0.1% Triton X-100) with 5% normal goat serum (NGS) and 2% FCS for 1 hour at room temperature. Subsequent incubation with primary antibodies diluted in PBS+ with 1% NGS and 1% FSC was performed overnight at 4°C. After extensive washing with PBS, cells/tissues were incubated with appropriate secondary antibodies and Hoechst for 1 hour at room temperature, washed with PBS, and mounted on glass slides. The following primary antibodies were used, directed against OCT4 (sc-5279; Santa Cruz Biotechnology, Santa Cruz, CA, http://www.scbt.com), SOX2 (#4900S; Cell Signaling Technology, Danvers, MA, http://www.cellsignal.com), NANOG (ab80892; Abcam, Cambridge, MA, http://www.abcam.com), SSEA-4 (Hybridoma Bank, http://dshb.biology.uiowa.edu; MC-813-70), TRA-1-60 (MAB4360; EMD Millipore, Billerica, MA, http://www.emdmillipore.com), TRA-1-81 (sc-21706; Santa Cruz Biotechnology), $\beta$IIItubulin (ab7751; Abcam), Desmin (M0760; Dako, Carpinteria, CA, http://www.dako.com), GATA4 (sc-25310; Santa Cruz Biotechnology), Nestin (MAB353; EMD Millipore), PAX6 (AB2237; EMD Millipore), OLIG2 (Tecan, http://www.tecan.com; 18953), NKX2.2 (Hybridoma Bank; 74.5A5), platelet-derived growth factor receptor-$\alpha$ (PDGFR$\alpha$) (sc-338; Santa Cruz Biotechnology), NG2 (AB5320; EMD Millipore), myelin proteolipid protein (PLP) (gift from the Department of Cell Biology University Medical Centre Groningen), MBP (AB980; EMD Millipore), NF (EnCor Biotechnology, Gainesville, FL, http://encorbio.com), CPCA-NF-H, hNuclei (MAB128; EMD Millipore), NF (RT97 & 2H3; DSHB), IBA-1 (019-19741; Wako, Osaka, Japan, http://www.wako-chem.co), CD11c (14-0114; eBioscience, San Diego, CA, http://www.ebioscience.com), CD3 (eBioscience; 14-0030), Ly-6C (MCA2389GA; AbD Serotec, Kidlington, U.K., http://www.abdserotec.com), glial fibrillary acidic protein (GFAP) (Z0334; Dako), GFP (MAB3580; EMD Millipore), Mac-2 (CL8942AP; Cedarlane Laboratories, Burlington, ON, Canada, http://www.cedarlanelabs.com), Ki67 (ab15580; Abcam), and STEM121 (AB-121-U-050; StemCells, Newark, CA, http://www.stemcellsinc.com). Tissue sections were also subjected to histochemical staining such as Luxol fast blue and cresyl violet to visualize myelin and general tissue composition, respectively. Quantification of immune cells in the EAE mice was done in standardized sections of multiple animals ($n$ = $\geq$4); quantification of implanted GFP-labeled hiPSC-derived OPCs in the marmoset was done by counting the number of positive cells in a minimum of five standard consecutive sections.

### Electron Microscopy

Sections were postfixed with 1% osmium tetroxide in 0.1 M sodium cacodylate for 2 hours at 4°C. The samples were washed with water, dehydrated through an ethanol series (30, 50, 70, 100%), and impregnated overnight in 1:1 Epon in ethanol. The diluted Epon was replaced by pure Epon and refreshed three times. Sections were embedded flat between two sheets of Aclar and polymerized at 58°C. With a stereomicroscope, 1 $\times$ 1-mm areas representing normal myelination, demyelination, and an implanted area were cut out and glued on an Epon stub. Ultrathin sections (70 nm) were cut using a Leica UC7 ultramicrotome (Leica, Amsterdam, The Netherlands, http://www.leica-microsystems.com) and contrasted with 2% uranylacetate in methanol and Reynolds lead citrate (2 minutes each). Images were acquired with a FEI Cm100 transmission electron microscope (FEI, Hillsboro, Oregon, http://www.fei.com) operated at 80 KV equipped with a Morada digital camera (Olympus Soft Imaging Solutions, Münster, Germany, http://www.olympus-sis.com).

## RESULTS

### Generation and Characterization of PSCs

We used skin fibroblasts from four healthy human donors to generate hiPSC lines. Fibroblast lines were transduced with a lentiviral polycistronic construct encoding for Oct4, Sox2, Klf4, and

fluorescent protein mCherry under the control of the EF1$\alpha$ promoter [17]. The efficiency of lentiviral transduction (nearly 100%) and subsequent silencing of exogenous genes was defined using an mCherry fluorescence marker. Of several emerging colonies, we picked two, further referred to in this paper as hiPSC colony 1 (Col1) and hiPSC colony 2 (Col2), and expanded them under feeder-free conditions. We extensively tested whether the selected clones met the well-established pluripotency criteria (Fig. 1B). Picked colonies showed typical human ESC-like morphology (Fig. 1B), expressed pluripotency-associated genes (Fig. 1B), and were able to differentiate in vitro into derivatives of the three germ layers (Fig. 1C). Moreover, we confirmed the pluripotency of the reprogrammed cells with the teratoma formation assay after subcutaneous injection in NOD-SCID mice (Fig. 1C). We observed no major differences between our two hiPSC lines (Col1 and Col2).

## Differentiation of hiPSCs Into Oligodendrocytes

We differentiated the two hiPSC lines into oligodendrocytes according to a modification of the protocol described for human ESCs by Hu et al. [18] (Fig. 1D: see details in Materials and Methods). At first, pluripotent cells were converted into embryoid bodies (EBs) that started to develop into early neuroepithelial cell clusters known as neural rosettes (Fig. 1D) after seeding on the substrate in neural differentiation-promoting medium. At this stage of differentiation, cells stained positive for the NSC markers PAX6 and nestin (Fig. 1D). Individual neural rosette structures were picked, mechanically dissociated, and cultured as suspension. At this stage, cell culture medium contained the growth factor bFGF and the morphogen SHH that allowed limited cell proliferation and conversion of cells into pre-OPCs characterized by the expression of the transcription factors OLIG2 and NKX2.2 (Fig. 1D). Maturation of pre-OPCs into OPCs was achieved by withdrawal of SHH from the culture medium and addition of a panel of growth factors and morphogens such as PDGF-AA, IGF-1, NT-3, and T3. At the end of this process, which lasted typically around 10 weeks, the formed oligospheres (clusters of OPCs) were seeded on laminin substrate, allowing OPCs to migrate out of the cell aggregates. Most of the migrating cells showed a typical multipolar OPC morphology (Fig. 1D) and were double-stained for specific OPC markers such as PDGFR$\alpha$/NKX2.2 and NG2/NKX2.2 (Fig. 1D). At this stage, the efficiency of differentiation was assessed by counting double-positive PDGFR$\alpha$/NKX2.2 cells. The efficiency varied between the two hiPSC lines and typically ranged from 45% (Col2) to 78% (Col1). Maturation of OPCs into functional oligodendrocytes was achieved by culturing them for another 2 to 3 weeks in growth factor-reduced conditions. OPCs were indeed able to develop into MBP- and PLP-positive oligodendrocytes (Fig. 1D); however, these highly specialized mature cells require very specific culture conditions, and most of them do not survive much beyond 3 weeks in the specific growth factor-reduced medium.

### Functionality of hiPSC-Derived OPCs In Vitro

To verify the proper differentiation and proper functionality of hiPSC-derived OPCs, we examined myelin formation in cocultures of hiPSC-derived OPCs with rat DRG neurons. Four weeks after plating, hiPSC-derived OPCs developed into mature, myelin-producing oligodendrocytes (supplemental online Fig. 1A) with a survival rate much higher than observed in monocultures lacking DRG neurons. High-magnification images revealed extensive myelination around the DRG axons, proving the myelin-forming capacity of the hiPSC-derived oligodendrocytes (supplemental online Fig. 1A).

### Functionality of hiPSC-Derived OPCs In Vivo

To examine and verify the (re)myelinating capacity of hiPSC-derived OPCs in vivo, we used the cuprizone mouse model. Mice were fed a 0.2% cuprizone-containing diet for 6 weeks before cell transplantation. Cuprizone causes selective oligodendrocyte death and extensive demyelination, particularly in the corpus callosum (supplemental online Fig. 1C); the bundles of nude axons in the corpus callosum provide a proper in vivo environment to examine remyelination activity by implanted OPCs. Three weeks after stereotactic grafting of hiPSC-derived cells (at the OPC stage of differentiation) (Fig. 1D) into the corpus callosum, animals were sacrificed and tissue was analyzed for the survival and fate of the implanted cells. Immunohistochemical staining of human nuclei revealed the presence of implanted cells mainly within the area of the corpus callosum (supplemental online Fig. 1D), traveling along the axonal tracks for distances $>$1 mm from the injection site. Double immunostaining and closer examination of the cell fate revealed that the implanted cells started to express MBP (supplemental online Fig. 1E). MBP/human nucleus double-staining was typically prominent for hiPSC-derived OPCs that migrated and settled along the axonal fibers of the corpus callosum, obtaining a thin, elongated nucleus morphology, typical for mature myelin-forming oligodendrocytes (supplemental online Fig. 1E). Similar observations were made after costaining for human nuclei and NF (supplemental online Fig. 1F): implanted OPCs, notably the ones with high migratory capacity that settled far from the injection site, obtained a thin, elongated nuclear morphology and became "squeezed in" between remyelinated axons (supplemental online Fig. 1F). Such close proximity to axons is one of the prerequisites for successful myelination. Part of the implanted hiPSC-derived OPCs did not (yet) differentiate into mature myelin-producing oligodendrocytes and retained OPC characteristics such as PDGFR$\alpha$ expression and an OPC-typical elongated, multipolar morphology (supplemental online Fig. 1F). The 3-week observation period may have been too short for them to migrate to their final destination and for further maturation. Finally, double staining for human nuclei and GFAP did reveal a few differentiated astrocytes among the implanted cells (supplemental online Fig. 1F). Quantification of implanted human cells coexpressing MBP, PDGFR$\alpha$, and GFAP revealed that the majority of the implanted cells were oligodendrocytes (supplemental online Fig. 1G).

In addition, we intended to validate the remyelinating capacity of the hiPSC-derived OPCs in EAE mice, representing the autoimmune inflammatory/demyelinating pathology of the chronic progressive form of MS. Immunization with MOG-peptide combined with complete Freund adjuvant results in the formation of lesions in the brain and the spinal cord, which give rise to clinical symptoms of which the severity is indicated by the EAE score. After intraventricular injection of the hiPSC-derived OPCs at the earliest detectable clinical symptoms, we observed a significant reduction of subsequent EAE scores in comparison with PBS-injected control mice (supplemental online Fig. 2B). Histochemical analysis of the EAE lesions in the cerebellum at day 36 after EAE induction revealed $CD3^+$, $CD11c^+$, and $Ly6C^+$ cell infiltrates and

 

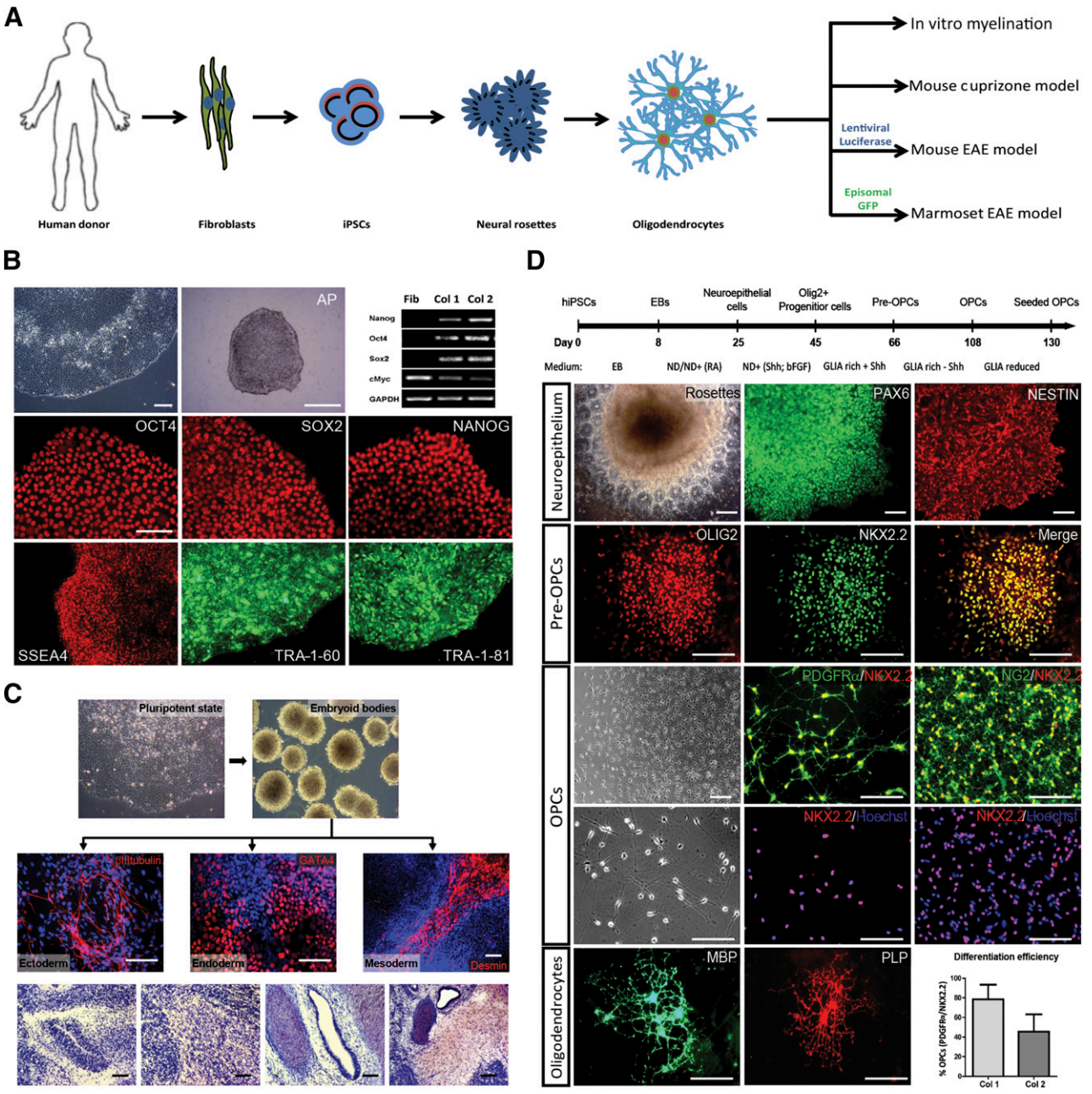


**Figure 1.** Generation of human iPSCs and their differentiation toward OPCs. **(A):** Schematic representation of the study setup. **(B):** Generation and characterization of hiPSC clones: phase-contrast image of hiPSC-colony, AP staining of hiPSC-colony, and RT-PCR analysis illustrating the endogenous expression of pluripotence-associated genes in reprogrammed cells; immunocytochemical detection of pluripotence-associated transcription factors (OCT4, SOX2, NANOG) and membrane markers (SSEA4, TRA-1-60, TRA-1-81). Scale bars: 50 $\mu$m; 500 $\mu$m for AP section. **(C):** In vitro and in vivo spontaneous differentiation of hiPSCs. In vitro, hiPSCs differentiated via EBs into ectoderm ($\beta$III-tubulin), endoderm (GATA4), and mesoderm (Desmin). In vivo differentiation of hiPSCs toward teratomas: hematoxylin and eosin staining of teratoma sections reveals the presence of neural, muscle, gland, and cartilage tissue. Scale bars: 50 $\mu$m; 200 $\mu$m for EB section. **(D):** Differentiation of hiPSCs into oligodendrocytes. Simplified scheme of differentiation protocol. Neuroepithelium: neural rosettes containing NSCs expressing PAX6 and NESTIN; pre-OPCs: immunostained for OLIG2 and NKX2.2; OPCs: phase-contrast image of OPCs migrating out of an oligosphere and (double) immunostainings for PDGFR$\alpha$/NKX2.2, NKX2.2/Hoechst, NG2/NKX2.2, and NKX2.2/Hoechst; oligodendrocytes: mature oligodendrocytes immunostained for MBP and PLP. Scale bars: 50 $\mu$m. Efficiency of iPSC to OPC differentiation: expressed as percentage of PDGFR$\alpha$/NKX2.2-positive cells of the total number of cells in one culture dish at the end of differentiation ($n$ = 3, $\pm$ SD) in two different hiPSC lines. Abbreviations: AP, alkaline phosphatase; bFGF, basic fibroblast growth factor; EAE, experimental autoimmune encephalomyelitis; EB, embryoid body; GFP, green fluorescent protein; hiPSC, human induced pluripotent stem cell; MBP, myelin basic protein; NSC, neural stem cell; OPC, oligodendrocyte precursor cell; PLP, myelin proteolipid protein; RA, rheumatoid arthritis; RT-PCR, reversetranscription-polymerase chain reaction.

demyelination (supplemental online Figs. 2E–2G, 3A). Comparing the cerebellum lesions of the EAE mice that received hiPSC-derived OPCs with those in PBS-treated control EAE mice revealed a significant reduction in cell infiltration in the hiPSC-derived OPC-treated mice (supplemental online Fig. 2E–2G). Iba-1 staining showed fewer activated microglia/macrophages in the hiPSC-

derived OPC-treated EAE mice compared with control PBS-treated EAE mice (supplemental online Figs. 2E, 4C). Moreover, the extent of demyelination was significantly less in the lesions of hiPSC-derived OPC-treated mice in comparison with the control PBS-treated mice (supplemental online Figs. 2C, 3), and fewer endogenous PDGFR$\alpha$-positive OPCs were present (supplemental online Fig. 4A, 4B). Decreased demyelination, however, could not be attributed to the activity of the implanted hiPSC-derived OPC, because no exogenous (grafted) cells could be detected in the lesions. IVIS bioluminescence scans corroborated that most of the grafted luciferase-labeled hiPSC-derived OPCs remained within the ventricles (supplemental online Fig. 2D). The beneficial effect of the grafted hiPSC-derived OPCs on the extent of cell infiltration and demyelination, and therefore on the resulting clinical score, is most likely caused by secreted factors, in line with previous observations that the beneficial effects of intraventricularly grafted NSCs in EAE mice and primates [19, 20] and of NSCs in spinal cord lesions [21] is mediated by secreted protective or anti-inflammatory factors [22]. We compared the expression of the most relevant secreted factors (such as CXCL10, CNTF, IGF1, VEGF, GDNF) by our hiPSC-derived OPCs with those of hiPSC-derived NSCs and found a similar profile (supplemental online Fig. 5). A major difference between hiPSC-derived OPCs and hiPSC-derived NSCs was the higher expression of hepatocyte growth factor, transforming growth factor-$\beta$, and interleukin-6 observed in the hiPSC-derived OPCs.

### Application of hiPSC-Derived OPCs in the Marmoset EAE Model for MS

After establishing the completeness of differentiation and proper functionality of hiPSCs-derived OPCs in vitro and in vivo, we examined the fate and functionality of hiPSCs-derived OPCs after stereotactical injection into a nonhuman primate model for MS. Immunization of unrelated common marmosets from an outbred colony with recombinant MOG peptides 34–56 in incomplete Freud's adjuvant activates a new pathogenic mechanism that elicits pathological features reminiscent of progressive MS, i.e., $CD8^+$ T cell-mediated demyelination in white matter, but also in cortical gray matter of the brain and progressive loss of neurological functions. The most prominent lesions containing severe demyelination and cell infiltration appear to be located within the corpus callosum (Fig. 2; supplemental online Fig. 6A). In a first pilot study (data not shown), we injected three EAE marmosets with hiPSC-derived OPCs into the CSF (cisterna magna) and sacrificed the monkeys after 7 days. Although we did observe localization of viable implanted cells in the ependymal cell layer that aligns the CSF, the entrance of the implanted cells into the brain parenchyma was slow and as yet minimal with this mode of administration. In the present study, we implanted GFP-labeled hiPSC-derived OPCs stereotactically near the medial line in the cortex just above the corpus callosum at day 79 (Fig. 3A–3C). Daily immunosuppressive treatment with cyclosporine A was started just before injection of the xenogenic grafts, to avoid interference with the development of EAE. Initially, we had planned to sacrifice the marmosets at 10, 20, 30, or 40 days after implantation. Unfortunately, the 10-day marmoset had to be sacrificed at day 3 for ethical reasons because it reached paresis (EAE score 2.5) a few days after implantation of the cells. Marmoset tissues were fixed and immunohistochemically examined for the fate of the implanted hiPSC-derived OPCs. Analysis of the GFP-labeled hiPSC-derived OPCs, at the different time points of injection in the four different animals, revealed the survival of these cells and their steady migration from the site of implantation mainly directed toward the large demyelinated lesions in the corpus callosum (Fig. 3). The number of implanted hiPSC-derived OPCs that could be detected in the corpus callosum after cortical injection increased with time (Fig. 3C, 3E and supplemental online Fig. 6B).

Migration across the corpus callosum occurred in both lateral and anterior/posterior directions from the site of injection, as was observed 40 days postimplantation (marmoset 4) (Fig. 3D). The double staining for MBP indicated that the GFP-labeled hiPSC-derived OPCs differentiated into myelin-producing cells (Fig. 4A). We performed costaining for MBP and NF as well as for MBP and GFP in subsequent serial sections (Fig. 4A) at 40 days after implantation (marmoset 4) and revealed interaction between the axons in the corpus callosum and the grafted hiPSC-derived OPCs (Fig. 4C). Costaining for MBP and STEM121 (human cytoplasmic marker) indicated that the hiPSC-derived OPCs differentiated into myelin-producing cells (Fig. 4B). PDGFR$\alpha$-GFP and Olig2-GFP double immunostaining at 40 days postimplantation showed that a substantial number of oligodendrocyte progenitors, along with MBP/GFP positive cells, resided in the corpus callosum (Fig. 4D; supplemental online Fig. 7C). However, after 40 days, a portion of PDGFR$\alpha$-GFP positive cells could still be detected at the site of injection (supplemental online Fig. 7A, 7B). The presence of a few GFAP-GFP double-positive cells indicated that astrocyte-like cells may have differentiated from the injected hiPSC-derived OPCs or may have contaminated the cell graft (Fig. 4D). Iba-1 and Mac2 immunostaining revealed the accumulation of microglia/macrophages around hiPSC-derived OPCs without compromising their viability (supplemental online Fig. 8A, 8B). Quantification for PDGFR$\alpha$-, GFAP-, MBP-, and Olig2-positive implanted ($GFP^+$) cells in one standard area within the corpus callosum revealed that most cells express OPC markers or have developed into mature MBP-positive cells (60%) 40 days after implantation.

To examine whether the implanted hiPSC-derived OPCs were capable of forming myelin sheets around axons in the lesions 40 days after implantation, we performed transmission electron microcopy. Tto identify the implanted cells in the EM sections, we performed 3,3′-diaminobenzidine-intensified immunostaining for GFP resulting in a clear, dark, very specific electron-dense precipitate in the entire cytoplasm under the EM microscope (Fig. 5A). Figure 5B shows in detail a GFP-positive (grafted) oligodendrocyte that wraps its extensions around a neighboring axon (indicated with a different color) in the lesion, forming a thin myelin sheet.

## Discussion

Human iPSC-derived OPCs have previously been shown to induce widespread and complete remyelination after transplantation into a mouse mutant (shiverer*)* that mimics human hypomyelinating leukodystrophies, genetic disorders in which myelin is not formed properly [9, 10]. Moreover, human iPSC-derived OPCs appeared capable of repairing radiation-induced myelin damage like that occurring in the clinic as a side effect of radiation therapy for pediatric brain cancers [12]. The relevance of both clinical applications for iPSC-derived OPCs may be considered limited. Genetic hypomyelinating leukodystrophies, such as Pelizaeus-Merzbacher disease, are rare [23], and for an effective treatment, autologous iPSC-derived OPCs (after gene correction) have to be administered

 

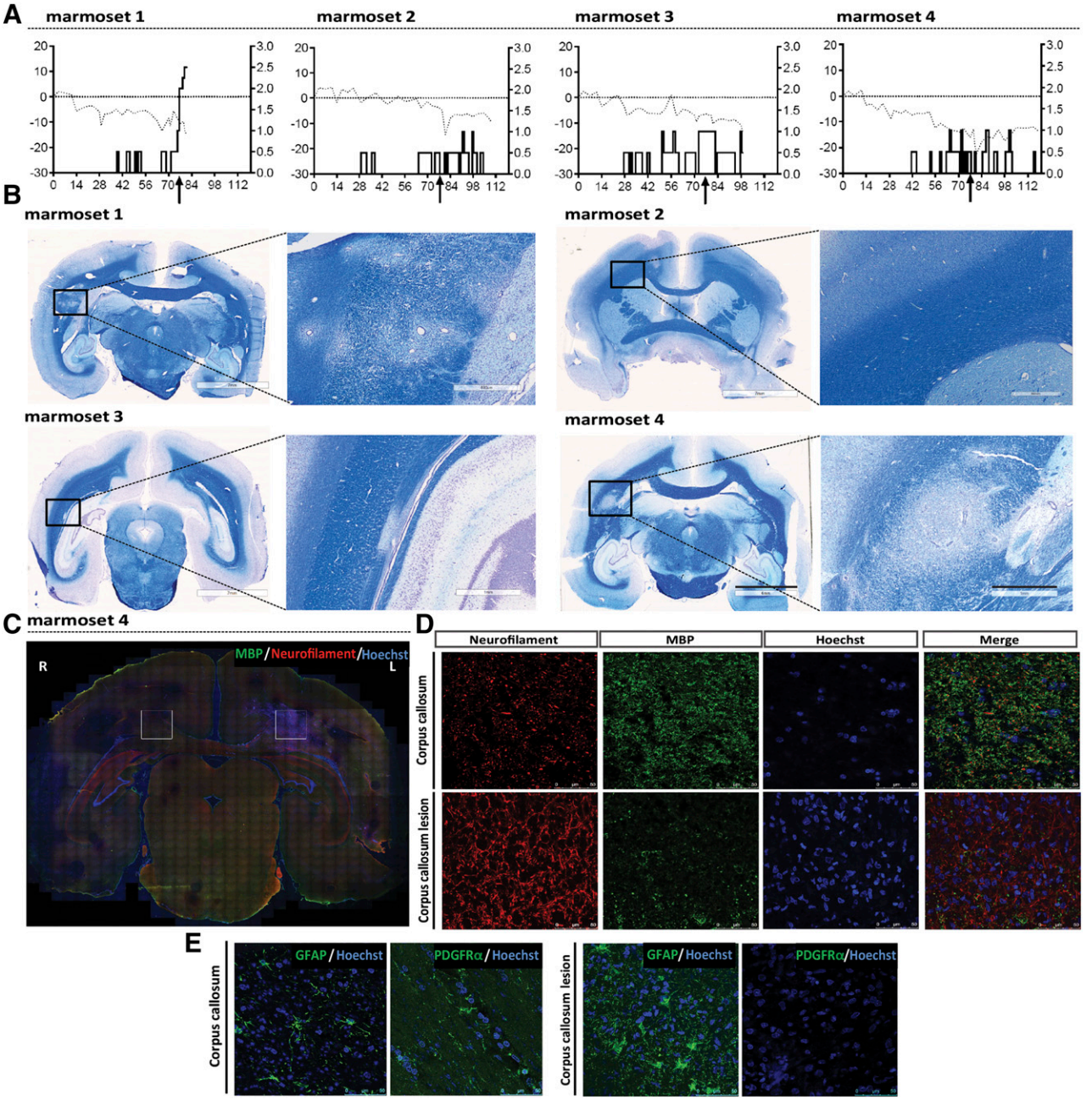


**Figure 2.** Marmoset EAE model. **(A):** Clinical score (right *y* axis) for EAE progression after MOG/IFA immunization, combined with body weight (left *y* axis, dotted line) in four marmosets. **(B):** Luxol fast blue staining reveals demyelinated lesions within the corpus callosum. Scale bars: 7 mm (overview), 1 mm and 500 $\mu$m (magnifications). **(C, D):** Neurofilament/MBP double immunostaining of a marmoset EAE brain section reveals a large lesion in the left corpus callosum; areas indicated by squares are further analyzed in C and D. **(E):** Immunostaining of the lesioned corpus callosum in the marmoset EAE brain shows morphologic changes in GFAP-positive astrocytes, absence of PDGFR$\alpha$-positive cells; loss of the myelin sheath (less MBP staining) results in the increased visibility of neurofilament-positive axons. Scale bars: 50 $\mu$m. Abbreviations: EAE, experimental autoimmune encephalomyelitis; GFAP, glial fibrillary acidic protein; IFA, incomplete Freund's adjuvant; MBP, myelin basic protein; MOG, myelin oligodendrocyte glycoprotein.

intrauterinely to successfully compete with the endogenous, affected, OPCs to produce normal myelin. Clinical application of autologous iPSC-derived OPCs after brain irradiation is relevant only in very young cancer patients, $<$0.5 years of age, when dividing OPCs, vulnerable to irradiation, may still be present.

However, the most common demyelinating disorder (incidence 1:1,000 in Western societies) and as such the most relevant target for an autologous iPSC-derived OPC transplantation therapy is MS. In the current nonhuman primate study we have shown for the first time that intracerebrally implanted human iPSC-derived OPCs survive for at least 40 days, albeit under immunosuppression with cyclosporine A, that they selectively migrate to MS-like lesions and are capable of initiating remyelination of denuded axons within the inflammatory conditions of these lesions. Our marmoset EAE model is generally considered the animal model that most closely mimics the secondary progressive

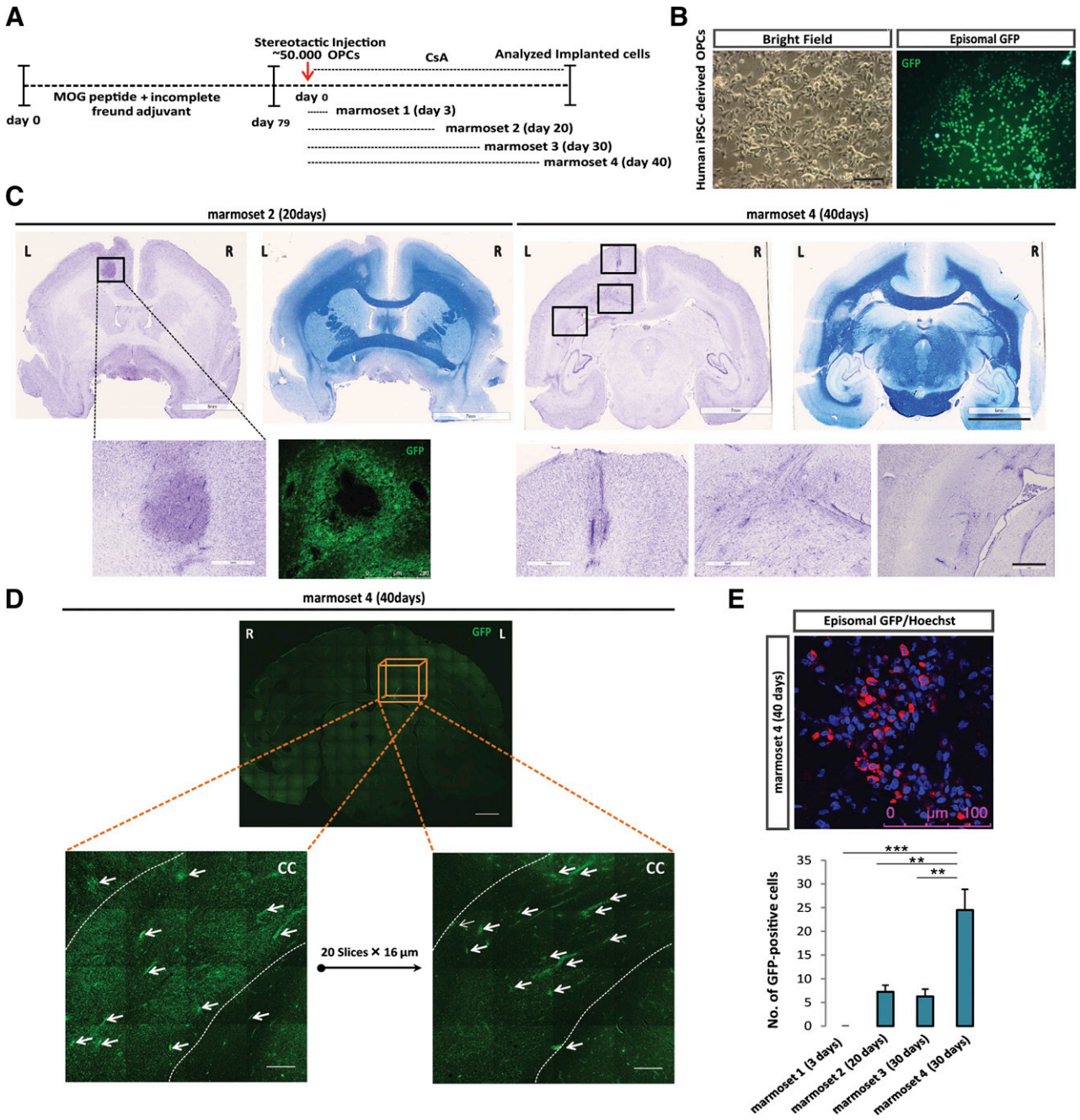


**Figure 3.** Implantation of human iPSC-derived OPCs in EAE marmosets. **(A):** Experimental setup for the implantation studies with human iPSC-derived OPCs in the marmoset EAE model. **(B):** Episomal GFP-transfected human iPSC-derived OPCs for implantation. Scale bar: 100 $\mu$m. **(C):** Cresyl violet and Luxol fast blue staining overview at 20 and 40 days after implantation depict the migration pattern of implanted cells in the EAE marmoset brain. Scale bars: 7 and 6 mm (whole brain) and 1 mm (magnification). **(D):** Analysis of two parallel sections, taken at a 320-$\mu$m interval, shows that GFP-labeled implanted cells migrate across the corpus callosum in both lateral and anterior/posterior directions. Scale bar: 2 mm (whole brain) and 250 $\mu$m (magnification). **(E):** Quantification of GFP-labeled implanted cells at a standard distance from the site of injection reveal the time-dependent pattern of migration (3, 20, 30, and 40 days) ($n = 4$, mean $\pm$ SEM, one-way analysis of variance; $*$, $p < .05$; $**$, $p < .01$; $***$, $p < .001$). Abbreviations: CC, corpus callosum; EAE, experimental autoimmune encephalomyelitis; GFP, green fluorescent protein; iPSC, induced pluripotent stem cell; MOG, myelin oligodendrocyte glycoprotein; OPC, oligodendrocyte precursor cell.

stage of MS in clinical and pathological presentation. The application of iPSC-derived OPCs is particularly relevant for MS patients in the secondary progressive stage, when endogenous OPCs are no longer able to remyelinate and rescue damaged axons and so prevent retrograde, irreversible neuronal degeneration. It is the most debilitating stage of the disease, for which no therapeutic treatment is yet available. We have injected iPSC-derived OPCs into the EAE marmosets during an early phase with functional endogenous OPCs still present. Moreover, because of the limited number of monkeys in this study, their outbred nature, the small stereotactically injected cell grafts, the relatively short posttransplantation period (because of animal care legislation imposed

 

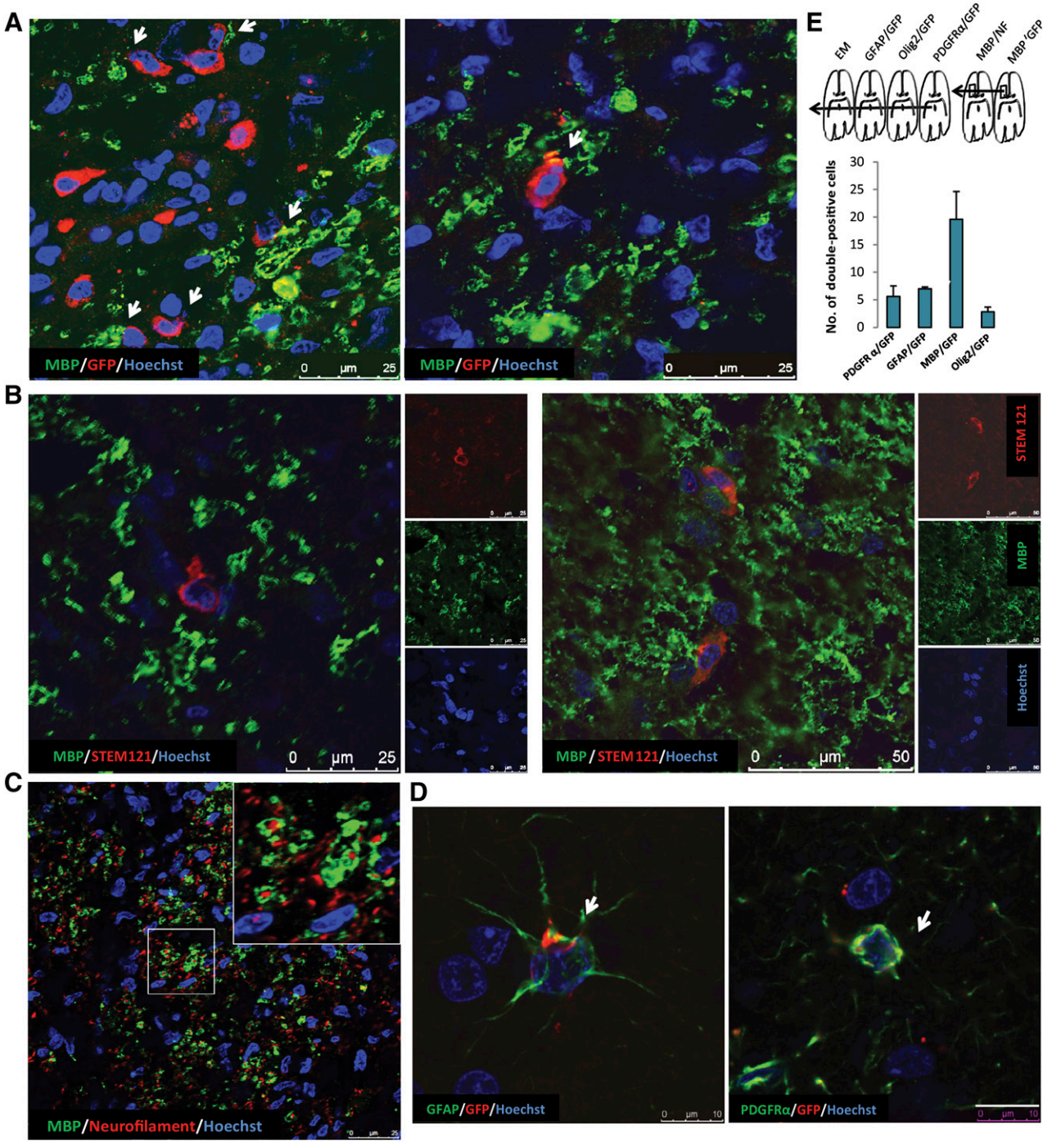


**Figure 4.** Analysis of hiPSC-derived OPCs in EAE marmosets. **(A):** GFP/MBP double immunostaining indicates that the implanted cells are capable of producing myelin. Scale bars: 25 $\mu$m. **(B):** STEM121/MBP double immunostaining indicates that the implanted cells are capable of producing myelin. Scale bars: 25 $\mu$m. **(C):** Neurofilament/MBP double immunostaining in the same area shows the close interaction of MBP-expressing implanted cells with unmyelinated axons. **(D):** Likewise, GFP/PDGFR$\alpha$ immunostaining reveals immature OPCs (arrows) among the implanted cells as well as a few GFP/GFAP double-stained cells (arrows), suggesting differentiation of the implanted cells toward astrocytes. Scale bars: 50 $\mu$m. **(E):** Scheme indicating the order of subsequent marmoset brain sections used for immunohistochemical analyses and electron microscopy studies. Quantification of PDGFR$\alpha$-, GFAP-, MBP-, and Olig2-positive implanted ($GFP^+$) cells in one standard area within the corpus callosum at 40 days after implantation indicates that the majority of implanted cells became MBP-positive oligodendrocytes. Data presented as mean $\pm$ SEM. Abbreviations: EAE, experimental autoimmune encephalomyelitis; EM, standard error of the mean; GFAP, glial fibrillary acidic protein; GFP, green fluorescent protein; hiPSC, human induced pluripotent stem cell; MBP, myelin basic protein; NF, neurofilament; OPC, oligodendrocyte precursor cell, PDGFR$\alpha$, platelet-derived growth factor receptor-$\alpha$.

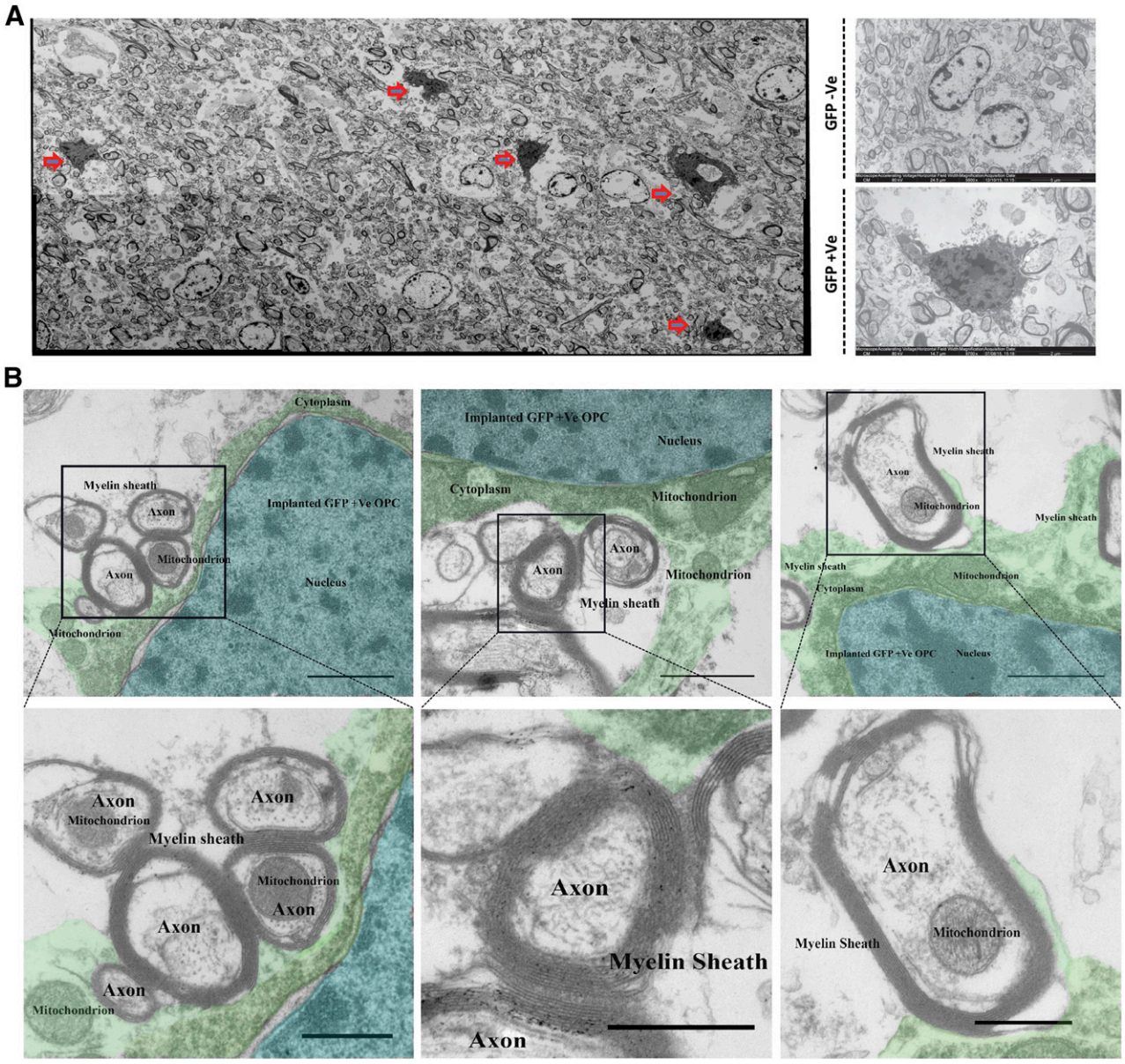


**Figure 5.** Electron microscopy of implanted human iPSC-derived OPCs in EAE marmosets. **(A):** Electron micrograph analysis of implanted hiPSC-derived OPCs (red arrows) in EAE marmoset brain based on DAB-intensified electron-dense GFP staining. **(B):** DAB-intensified electron-dense GFP-labeled oligodendrocytes myelinate multiple axons in the EAE lesion in the marmoset brain (blue, nucleus; green, cytoplasm). Scale bars: 500 nm. Abbreviations: DAB, 3,3′-diaminobenzidine; EAE, experimental autoimmune encephalomyelitis; GFP, green fluorescent protein; hiPSC, human induced pluripotent stem cell; OPC, oligodendrocyte precursor cell; +Ve, positive; –Ve, negative.

restrictions) and the usage of cyclosporine A, firm conclusions about the consequences of iPSC-derived OPC transplantation for clinical improvement could not be drawn as yet. Nevertheless, extrapolation of the beneficial effect of the iPSC-derived OPCs observed in the mouse EAE model to the EAE model in marmosets, warrants the assumption that under comparable experimental conditions a clinical effect is likely.

Previous studies have shown that rodent NSCs and OPCs produce a variety of immunomodulatory, anti-inflammatory, and neurotrophic factors, responsible for a significant reduction in clinical scores in EAE animals after intraventricular or intravenous injection [20, 22, 24–27]. In addition, neuroprotective effects of the secretome of NSCs have been demonstrated after spinal cord injury in mice [21] and after intracerebellar injection of NSCs in mouse models of Machado-Joseph disease [28]. The responsible factors in the secretome of NSCs and OPCs have been determined [22, 29–31]. Also in this study, human iPSC-derived OPCs appeared to express a similar set of factors and were able to reduce the EAE clinical score in mice after intraventricular injection, mainly by reducing cell infiltration and lesion size. In particular, leukemia inhibitory factor (LIF) secreted by mouse NSCs or OPCs has been proposed as playing a crucial neuroprotective and inflammation suppressive role in the EAE mouse model [32, 33]. However, our analyses show that LIF production by human NSCs and human OPCs, in contrast to mouse NSCs and human OPCs, is only at a low basic level, suggesting that other factors secreted by human

 

OPCs might play a more prominent neuroprotective role. The local stereotactical injection of human iPSC-derived OPCs in the marmoset cortex did not provoke a reduction in clinical scores, most likely because of only a very limited, local diffusion of the effectors (in contrast to the more systemic intraventricular or intravenous administration in EAE mice).

## Conclusion

Our results show for the first time efficacious remyelination of hiPSC-derived OPCs in primates with MS-like disease, which represents the closest possible approximation to the human situation. Although the results are very encouraging, they also immediately point to required follow-up experiments addressing the optimal mode of administration that will allow migration of sufficient hiPSC-derived OPCs to multiple lesion sites. Some of these sites may be less accessible, e.g., when they are clinically silent, with only a low release of chemotactic factors attracting the implanted iPSC-derived OPCs and/or enclosed by an astrocytic scar. In view of the current safe possibilities to genetically modify human iPSC-derived cells, the hiPSC-derived OPCs may be equipped with additional chemokine receptors and/or enzymes that degrade the astrocytic scar. Long-term studies will be essential to determine the safety and stability of grafted iPSC-derived OPCs. Moreover, it will be interesting to evaluate whether remyelination capacity and immune modulation by hiPSC-derived OPCs may be of therapeutic use for primary progressive MS.

Some concern may exist about the safe, large-scale production of autologous iPSCs and iPSC-derived OPCs and the time and costs associated with it. The wide-scale implementation of haplotype-based banking of readily available, well-characterized human iPSCs (fulfilling cGMP criteria) for transplantation, may eventually obsolete the need to generate iPSC lines for each individual MS patient [34, 35]. Moreover, recent improvements in the protocol for the differentiation of human iPSCs into OPCs have led to a significant reduction in the duration of this procedure [36, 37]. Finally, in a recent report, Rao and Atala have proposed important steps to reduce the costs for iPSC production significantly [38].

## Acknowledgments

We thank Divya Raj, Zhuoran Yin, and Michel Meijer for help with imaging. This work was supported by the Dutch MS Research Foundation, grants MS08-637 and MS09-694. Part of this work was supported by EUPRIM-Net under EU Contract 262443 of the 7th Framework Program. Part of the work was performed at the University Medical Centre Groningen Imaging and Microscopy Center, which is sponsored by Netherlands Organisation for Scientific Research (NWO) Grant ZonMW 91111.006.

## Author Contributions

A.T. and M.C.: performance of research, formulation of hypothesis and initiation and organization of study, experiment design and data analysis, manuscript writing or contribution; Y.A.K., J.K., and M.B.: experiment design and data analysis, contributions to specific experiments and analyses; I.M.-O.: contributions to specific experiments and analyses, manuscript writing or contribution; I.V.: contributions to specific experiments and analyses; W. Baron: experiment design and data analysis; B.G.: experiment design and data analysis, manuscript writing or contribution; W. Brück: formulation of hypothesis and initiation and organization of study, experiment design and data analysis; B.A.t.H. and E.B.: formulation of hypothesis and initiation and organization of study, experiment design and data analysis, manuscript writing or contribution; S.C.: formulation of hypothesis and initiation and organization of study, experiment design and data analysis, manuscript writing or contribution, supervision and final editing of manuscript.

## Disclosure of Potential Conflicts of Interest

The authors indicated no potential conflicts of interest.

## References

1 Hauser SL, Chan JR, Oksenberg JR. Multiple sclerosis: Prospects and promise. Ann Neurol 2013;74:317–327.

2 Hemmer B, Archelos JJ, Hartung HP. New concepts in the immunopathogenesis of multiple sclerosis. Nat Rev Neurosci 2002;3:291–301.

3 Stys PK, Zamponi GW, van Minnen J et al. Will the real multiple sclerosis please stand up? Nat Rev Neurosci 2012;13:507–514.

4 Goldman SA, Nedergaard M, Windrem MS. Glial progenitor cell-based treatment and modeling of neurological disease. Science 2012; 338:491–495.

5 Uchida N, Chen K, Dohse M et al. Human neural stem cells induce functional myelination in mice with severe dysmyelination. Sci Transl Med 2012;4:155ra136.

6 Takahashi K, Yamanaka S. Induction of pluripotent stem cells from mouse embryonic and adult fibroblast cultures by defined factors. Cell 2006;126:663–676.

7 Ogawa S, Tokumoto Y, Miyake J et al. Induction of oligodendrocyte differentiation from adult human fibroblast-derived induced pluripotent stem cells. In Vitro Cell Dev Biol Anim 2011;47:464–469.

8 Pouya A, Satarian L, Kiani S et al. Human induced pluripotent stem cells differentiation into oligodendrocyte progenitors and transplantation in a rat model of optic chiasm demyelination. PLoS One 2011;6:e27925.

9 Wang S, Bates J, Li X et al. Human iPSC-derived oligodendrocyte progenitor cells can myelinate and rescue a mouse model of congenital hypomyelination. Cell Stem Cell 2013; 12:252–264.

10 Douvaras P, Wang J, Zimmer M et al. Efficient generation of myelinating oligodendrocytes from primary progressive multiple sclerosis patients by induced pluripotent stem cells. Stem Cell Rep 2014;3:250–259.

11 Najm FJ, Madhavan M, Zaremba A et al. Drug-based modulation of endogenous stem cells promotes functional remyelination in vivo. Nature 2015;522:216–220.

12 Piao J, Major T, Auyeung G et al. Human embryonic stem cell-derived oligodendrocyte progenitors remyelinate the brain and rescue behavioral deficits following radiation. Cell Stem Cell 2015;16:198–210.

13 Franklin RJ, Ffrench-Constant C. Remyelination in the CNS: From biology to therapy. Nat Rev Neurosci 2008;9:839–855.

14 Jagessar SA, Kap YS, Heijmans N et al. Induction of progressive demyelinating autoimmune encephalomyelitis in common marmoset monkeys using MOG34-56 peptide in incomplete Freund adjuvant. J Neuropathol Exp Neurol 2010;69:372–385.

15 't Hart BA, Hintzen RQ, Laman JD. Preclinical assessment of therapeutic antibodies against human CD40 and human interleukin-12/23p40 in a nonhuman primate model of multiple sclerosis. Neurodegener Dis 2008;5:38–52.

16 Palazzi X, Bordier N. The marmoset brain in stereotaxic coordinates. New York: Springer-Verlag, 2008.

17 Sommer CA, Stadtfeld M, Murphy GJ et al. Induced pluripotent stem cell generation using a single lentiviral stem cell cassette. Stem Cells 2009;27:543–549.

18 Hu Z, Li T, Zhang X et al. Hepatocyte growth factor enhances the generation of high-purity oligodendrocytes from human embryonic stem cells. Differentiation 2009;78: 177–184.

19 Pluchino S, Gritti A, Blezer E et al. Human neural stem cells ameliorate autoimmune encephalomyelitis in non-human primates. Ann Neurol 2009;66:343–354.

**20** Sher F, Amor S, Gerritsen W et al. Intraventricularly injected Olig2-NSCs attenuate established relapsing-remitting EAE in mice. Cell Transplant 2012;21:1883–1897.

**21** Sabelström H, Stenudd M, Réu P et al. Resident neural stem cells restrict tissue damage and neuronal loss after spinal cord injury in mice. Science 2013;342:637–640.

**22** Pluchino S, Cossetti C. How stem cells speak with host immune cells in inflammatory brain diseases. Glia 2013;61:1379–1401.

**23** Numasawa-Kuroiwa Y, Okada Y, Shibata S et al. Involvement of ER stress in dysmyelination of Pelizaeus-Merzbacher Disease with PLP1 missense mutations shown by iPSC-derived oligodendrocytes. Stem Cell Rep 2014;2: 648–661.

**24** Einstein O, Grigoriadis N, Mizrachi-Kol R et al. Transplanted neural precursor cells reduce brain inflammation to attenuate chronic experimental autoimmune encephalomyelitis. Exp Neurol 2006;198:275–284.

**25** Cossetti C, Alfaro-Cervello C, Donegà M et al. New perspectives of tissue remodelling with neural stem and progenitor cell-based therapies. Cell Tissue Res 2012;349:321–329.

**26** Donega M, Giusto E, Cossetti C et al. Systemic injection of neural stem/progenitor cells in mice with chronic EAE. J Vis Exp 2014 [Epub ahead of print].

**27** Cusimano M, Biziato D, Brambilla E et al. Transplanted neural stem/precursor cells instruct phagocytes and reduce secondary tissue damage in the injured spinal cord. Brain 2012; 135:447–460.

**28** Mendonça LS, Nóbrega C, Hirai H et al. Transplantation of cerebellar neural stem cells improves motor coordination and neuropathology in Machado-Joseph disease mice. Brain 2015;138:320–335.

**29** Drago D, Cossetti C, Iraci N et al. The stem cell secretome and its role in brain repair. Biochimie 2013;95:2271–2285.

**30** Kim WK, Kim D, Cui J et al. Secretome analysis of human oligodendrocytes derived from neural stem cells. PLoS One 2014;9:e84292.

**31** Pluchino S, Zanotti L, Rossi B et al. Neurosphere-derived multipotent precursors promote neuroprotection by an immunomodulatory mechanism. Nature 2005;436: 266–271.

**32** Cao W, Yang Y, Wang Z et al. Leukemia inhibitory factor inhibits T helper 17 cell differentiation and confers treatment effects of neural progenitor cell therapy in autoimmune disease. Immunity 2011;35:273–284.

**33** Laterza C, Merlini A, De Feo D et al. iPSC-derived neural precursors exert a neuroprotective role in immune-mediated demyelination via the secretion of LIF. Nat Commun 2013;4:2597–2613.

**34** Nakatsuji N, Nakajima F, Tokunaga K. HLA-haplotype banking and iPS cells. Nat Biotechnol 2008;26:739–740.

**35** Zimmermann A, Preynat-Seauve O, Tiercy JM et al. Haplotype-based banking of human pluripotent stem cells for transplantation: potential and limitations. Stem Cells Dev 2012; 21:2364–2373.

**36** Fossati V, Douvaras P. Generating induced pluripotent stem cells for multiple sclerosis therapy. Regen Med 2014;9:709–711.

**37** Douvaras P, Fossati V. Generation and isolation of oligodendrocyte progenitor cells from human pluripotent stem cells. Nat Protoc 2015;10:1143–1154.

**38** Rao MS, Atala A. Developing induced pluripotent stem cell-based therapy for the masses. STEM CELLS TRANSLATIONAL MEDICINE 2016;5:129–131.

See www.StemCellsTM.com for supporting information available online.

 